RSC Advances

ROYAL SOCIETY OF CHEMISTRY

www.rsc.org/advances

This device can detect and discriminate toxic and non-toxic gases in the ppb level at room temperature.

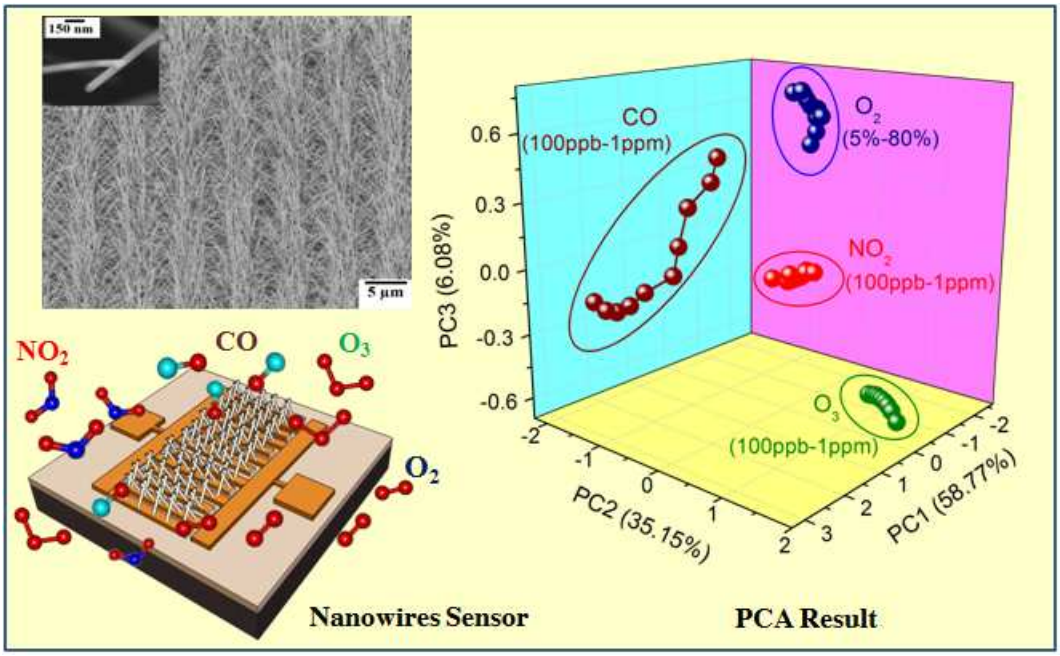

Electronic Nose for Toxic Gas Detection based on Photostimulated Core-Shell Nanowires

Chatchawal Wongchoosuk[1,2,*], Kittitat Subannajui[2,3], Chunyu Wang[4], Yang Yang[2,5], Firat Güder[2,6], Teerakiat Kerdcharoen[7], Volker Cimalla[4], Margit Zacharias[2]

[1]Department of Physics, Faculty of Science, Kasetsart University, Bangkok 10900, Thailand

[2]Laboratory for Nanotechnology, Institute of Microsystems Engineering (IMTEK), Albert Ludwigs University, Freiburg 79110, Germany

[3]Material science and Engineering Program, Faculty of Science, Mahidol University, Bangkok 10400, Thailand

[4]Fraunhofer-Institute for Applied Solid-State Physics, Freiburg 79108, Germany

[5]State Key Laboratory of Materials-Oriented Chemical Engineering, College of Chemistry and Chemical Engineering, Nanjing Tech University, Nanjing 210009, China

[6]Whitesides Research Group, Department of Chemistry and Chemical Biology, Harvard University, Cambridge, Massachusetts 02138, United States

[7]Department of Physics, Faculty of Science, Mahidol University, Bangkok 10400, Thailand

***Corresponding author>>** E-mail: chatchawal.w@ku.ac.th

Tel.: +662-562-5555; Fax: +662-942-8029

Abstract

A novel fabrication of microelectronic nose based on ZnO nanowires and ZnO surface modifications including ZnO-$ZnAl_2O_4$ core-shell nanowires and ZnO-Zn_2TiO_4 core-shell nanowires gas-sensing elements operated at room temperature is reported. By combining vapor-phase transport processes and atomic layer deposition techniques, highly homogeneous core-shell nanowires structures can be successfully obtained on large scale areas. Under ultraviolet illumination on the specific oxide surfaces, photo-stimulated oxygen species ($O_2^-(ads)$) response and dominate the gas sensing mechanism of the core-shell nanowires at room temperature. Principal component analysis results show the perfect discrimination of gases including toxic gases and non-toxic gases. This novel device can be used to identify both the gas type and the concentration of the gases with concentrations in the ppb level at room temperature.

Keywords: E-nose, Gas Sensor, 1D Nanostructures, ZnO, Kirkendall Effect

1. Introduction

Since more than a decade, so-called electronic nose (E-nose) became a very well-known practical device for sensing technology. With the ability to identify many detecting substances, E-noses are now widely used in several branches of science and engineering, for examples, biosensor E-nose, gas sensor E-nose, or liquid sensor E-nose [1-5]. Although originally it was created in analogy to 'a nose', the application of E-nose is far better than a natural nose in term of quantity analysis. Furthermore E-nose can be used to characterize a substance which might endanger humans.

A normal E-nose is composed of an array of sensors which usually has thin films as sensing receptors. Recently instead of using thin films, E-nose based on nanowires is in the focus of attention. The superior properties in 1D-nanostructure such as a higher surface per volume ratio, potential band-depletion, and surface charge accumulation can provide a better sensitivity with lower power consumption [6]. Therefore, attempts to produce nanowires based E-nose have been increasing. In order to fabricate nanowires sensor arrays, sets of sensors based on different materials are normally combined. An example was shown for instance by Chen et al. [7]. Carbon nanotubes, In_2O_3, SnO_2 and ZnO nanowires were used to act as different selective sensing material on the same E-nose platform. Baik et al. demonstrated a method to obtain an E-nose from a single material, i.e. SnO_2 nanowires, with different metallic decorations on the surface [8]. Despite of the progress accomplished, most of nanowires E-nose still requires high operating temperatures (>200 ◦C). In this paper, we report the development of photo-stimulated E-nose based on pristine ZnO nanowires and surface reconstruction of ZnO nanowires including ZnO-$ZnAl_2O_4$ core-shell and ZnO-Zn_2TiO_4 core-shell nanowires that work at room temperature for

detecting toxic gases. The sensing mechanism of the core-shell nanowires under photo-activation will be discussed in details.

2. Experimental details

The fabrication of the respective ZnO nanowires based E-nose started with the preparation of a 100 nm dry oxide (SiO_2) as insulated layer on a Si wafer accomplished in the usual way. The Cr (5 nm): Au (100 nm) interdigitated electrode array (IDA) with comb-like pattern was then fabricated on the insulator by conventional photolithography. The produced IDA was cleaned with acetone, isopropanol, and deionized water, and was dried with N_2. In order to establish the sensing materials, ZnO nanowires were directly grown on the IDA by vapor-phase transport process. Note that the ZnO nanowires selectively grow on the lithographically structured Au layer of IDA while the density and thickness of the ZnO nanowires can be well controlled by fixed optimum growth conditions [9]. Briefly, a mixture of ZnO (purity 99.999%, Sigma–Aldrich) and graphite (−200 mesh, purity 99.9995%, Alfa Aesar) powders in a 1:1 ratio by weight was placed at the 950 °C position of the horizontal (vacuum tight) two-zone the furnace as vapor source and the IDA at the 750 °C position as substrate. The nanowires synthesis was carried out at 30 mbar under a constant flow rate of 30 sccm Ar (99.9999%) and 1.5 sccm Ar/O_2 mixture (Ar/O_2 ration of 90/10, purity 99.999%) for 20 min. By vapor phase deposition, the ZnO nanowires grew densely and perpendicular or slightly tilted on the electrodes. Hence, at the interdigitated pads, the ZnO nanowires grow across the electrodes with many touching points air-bridged between the nanowires from adjacent contact pads forming a metal-semiconductor-semiconductor-metal device. The sensing of ZnO nanowires results from resistance modulation of the ZnO nanowires across two electrodes as shown in the

schematic device in Fig. 1a. To further establish different sensing materials, the ZnO nanowires were coated homogeneously with 5 nm oxides such as Al_2O_3 and TiO_2 by atomic layer deposition (ALD) to obtain core-shell nanostructures. The Al_2O_3 and TiO_2 were formed at 115 °C by reacting trimethylaluminum or titanium isopropoxide, respectively, with water vapor in a vertical flow type reactor (OpAL, Oxford Instruments). The coated samples were subsequently annealed at 700 °C for 3 h to achieve $ZnAl_2O_4$ or Zn_2TiO_4 on the surface of ZnO nanowires, respectively, based on solid-state reactions [10].

All three nanowires gas sensors including the ZnO, ZnO-$ZnAl_2O_4$ core-shell, and ZnO-Zn_2TiO_4 core-shell nanowires sensing parts were used to characterize toxic and non-toxic gases at room temperature. An ultraviolet (UV) light-emitting diode (LED) with $\lambda \sim 356$ nm and optical power ~ 200 μW was mounted above the sensors for photostimulation. The gas sensor array will be later integrated on the handling printed circuit board (PCB) for an E-nose. Before introducing gases into the measuring chamber, the chamber was evacuated down to ~10^{-3} mbar, followed by purging of sythesized air. This cycle was repeated several times. After that, different gases, such as O_3, CO and NO_2 with a concentration between 100 ppb and 1 ppm and O_2 with a concentration of 5% to 80% in nitrogen were individually led into the chamber adjusted by mass flow controller. During sensing, the UV LED was switched off in present of target gases and was switched on when the target gas was removed. Theoretically, a large photocurrent will be induced by switching on/off the above-band-gap excitation due to photogenerated carriers [11]. The resistance minima in absent of target gas (R_0) and maxima in target gas (R_G) of the nanomaterials were recorded. The response of the sensor (S) is defined as ($S= |(R_G-R_0)/R_0| \times 100\%$). Next, the sensor response data from all sensors were introduced into principal component analysis (PCA) to provide classification/qualification results of the sensors upon toxic and non-

toxic gases. The PCA is a multivariate technique that transforms the overall information into a set of new linear combinations of orthogonal variables called principal components (PC) without heavy loss of important original information.

3. Results and Discussion

The electrode was designed with a gap size between adjacent electrodes of 3 μm as shown in the inset of Fig. 1b. After the growth of ZnO nanowires, adjacent electrodes are electrically connected by cross ZnO nanowires (see Fig. 1c). The diameter and length of ZnO nanowires are in the range of 60-180 nm and a few tens of μm, respectively. As one can see in the inset of Fig. 1c, the ZnO nanowires are self-assembled between the gaps of electrodes. This electrical connection by a simple self-assembly process during synthesis reduces tedious and time consuming task comparing with other nanowire-based gas sensor fabrication techniques [12-14]. With the growth condition used here in our vapor phase deposition chamber, the density of ZnO nanowires is also well-controlled. The nanowires are single-crystalline with the typical [0002] elongation (*c*-oriented) and follow the vapor–solid (VS) growth mechanism as shown in Fig. 2a.

To investigate formation of ZnO-$ZnAl_2O_4$ core-shell and ZnO-Zn_2TiO_4 core-shell nanowires, Figure 2b and 2c present the transmission electron microscope (TEM) images of structures after annealing ZnO-Al_2O_3 and ZnO-TiO_2 nanowires under identical conditions. For ZnO-$ZnAl_2O_4$ core-shell nanowires, cavities distributed along the interface clearly show the existence of bridge-like linkages between the residual ZnO core and the spinel $ZnAl_2O_4$ shell (see Fig. 2b) after solid-solid reaction. The one-way interfacial bulk diffusion of ZnO into the amorphous Al_2O_3 shell can form the $ZnAl_2O_4$ at shell and generate a series of cavities at the

interface due to the Kirkendall effect [10]. Unlike the reaction of ZnO-Al_2O_3 nanowires, no cavity was observed at ZnO-Zn_2TiO_4 core-shell interface (see Fig. 2c), indicating the interdiffusion between ZnO and TiO_2 was not dominated by the Kirkendall effect in this case. Apparently, from the electron diffraction (ED) patterns, the unreacted ZnO nanowires cores still keep the single-crystal nature while the formed $ZnAl_2O_4$ and Zn_2TiO_4 are polycrystalline with a rough surface feature.

It is well known that the gas sensitivity of ZnO nanowires comes from the trapping of the gas molecules on the surface which can modulate the surface depletion layer width [15]. The negative charges at the surface of n-type semiconductor usually generate an upward electronic band-bending along the diameter of ZnO nanowires [16]. The surface charges influence the surface-band potential and cause a stronger or a weaker band-bending. This modulation of band-bending directly makes a change in the conduction of ZnO nanowires. Figure 3 demonstrates the dynamic responses of nanowires sensors to oxidizing NO_2 gas at room temperature under on/off UV illumination cycles. The electrical resistance of all the sensors increases at the moment of NO_2 exposure. By applying UV illumination, electron–hole pairs are generated in sensing materials. The photo-generated holes can migrate to the surface via the electric field induced by the band bending and react with adsorbed oxygen species ($O_2^-(ads)$). At the same time, the photo-generated electrons react with additional photoinduced oxygen ions, resulting to form photostimulated oxygen species ($O_2^-(ads)$) at the shell surfaces as the following schemes [17]:

$$h\nu \rightarrow h^+(h\nu) + e^-(h\nu) \quad (2)$$

$$h^+(h\nu) + O_2^-(ads) \rightarrow O_2(g) \quad (3)$$

$$O_2(g) + e^-(h\nu) \rightarrow O_2^-(h\nu) \quad (4)$$

Upon exposure to NO_2, NO_2 molecules come to react with the photostimulated oxygen species on the surface to capture available free electrons in the following reaction:

$$NO_2(g) + O_2^-(hv) + 2e^-(hv) \rightarrow NO_2^-(ads) + 2O^-(ads) \quad (5)$$

This reaction increases the concentration of holes that enlarged the band bending, leading to an increase of depletion layer width. Therefore, resistance of core-shell nanowire sensor increases with increasing NO_2 concentration. Moreover, NO_2 can also directly capture the electrons from the conduction band due to its higher electrophilic properties [18].

From Fig. 4, at low NO_2 concentrations (100-300 ppb), the ZnO-Zn_2TiO_4 core-shell nanowires sensor shows high response to NO_2 over other sensors (more than 50%) due to more surface roughness for specific NO_2 adsorptions while it also shows medium sensitivity to O_2 and relatively low sensitivity to CO and O_3. At concentration of 100 ppb, the gas responses of ZnO-Zn_2TiO_4 core-shell nanowires sensor to NO_2 and CO are ~109 and ~96, respectively. For the ZnO nanowires sensor, it is sensitive to most of gases. Especially, upon exposure to O_3, the signal of ZnO nanowires sensor always reaches to saturation point. The cross-sensitivity problem makes its selectivity of ZnO nanowire to be low. This may provide an ambiguous response in terms of individual components of the gas mixtures. In case of ZnO-$ZnAl_2O_4$ core-shell nanowires, it exhibits high sensitivity and selectivity to NO_2. At concentration of 1 ppm, the gas responses of ZnO-$ZnAl_2O_4$ core-shell nanowires sensor to NO_2, CO, and O_3 are ~ 137, 38, and 44, respectively. Moreover, its response to O_2 with a concentration of 5-80% in nitrogen is in range of only 32-45. This refers to the good performance for NO_2 detection in real world application. The NO_x species prefer to adsorb on the $ZnAl_2O_4$ surface over other gases via π^*(N) transitions [19]. Enhancement of sensing properties of core-shell nanowires over ZnO nanowires may result from the contribution of n−n heterojunction that can adjust energy barrier

height and modulate electron transport [20]. In comparison between ZnO-Zn_2TiO_4 and ZnO-$ZnAl_2O_4$ core-shell nanowires, the different sensing properties cause from different rough surface feature and intrinsic material properties. The rough surface feature of the ZnO-Zn_2TiO_4 improves the efficiency and the amount of oxygen chemisorptions [21] resulting in an enhancement of gas responses on all target gases over the ZnO-$ZnAl_2O_4$. The Al_{Zn} antisite defects in $ZnAl_2O_4$ spinel were found to act as a shallow donor and Al-O bond appears more ionic [22]. This can contribute to charge transports between NO_2 and ZnO-$ZnAl_2O_4$ core-shell nanowires leading to higher selectivity of the ZnO-$ZnAl_2O_4$ core-shell towards NO_2.

To evaluate the discrimination power of core-shell sensor array, the PCA was carried out with the relative response feature extraction technique [2]. As shown in Fig. 5, the PCA result is clearly separated to 4 clusters corresponding to the 4 different target gases. No overlap between different gas species occurs in PCA. It indicates the high performance of such nanowires gas sensor array for detection and discrimination of both oxidizing and reducing gases at room temperature over other pervious work that usually operated at high temperatures (>200 ◦C) [7, 23]. Here we demonstrate that the nanowires E-nose based on ZnO nanowires and surface modification can be used to identify both gas type and the concentration of gases at room temperature. This device will be very useful in term of energy conservation.

4. Conclusion

In summary, we propose a simple but reliable method for the nanowires E-nose fabrication. The E-nose composed of three nanowires sensors which are ZnO nanowires, ZnO-$ZnAl_2O_4$ core-shell nanowires, and ZnO-Zn_2TiO_4 core-shell nanowires. The photolithography was used to pattern and identify the ZnO nanowires structure. The ZnO nanowires were grown

by vapor phase deposition and the result from the growth is the cross nanostructure of ZnO nanowires between two electrodes. The sensor array was then deposited by ALD before annealing process. After an annealing at 700 ^{o}C, the solid reactions were completed. All three sensors were used to sense NO_2, CO, O_2, and O_3 at room temperature. Based on photostimulation by UV, oxygen species (O_2^-) can be generated to adsopt on the nanowires surface for interacting with gas molecules. The results show that pure ZnO nanowires cannot use as a potential single gas sensor for detection of toxic gas in real envelopment at room temperature due to cross sensitive problem of ZnO surface. The $ZnAl_2O_4$ surface shows high sensitivity and selectivity to NO_2 while Zn_2TiO_4 exhibits improvement of gas response of toxic gas (NO_2 and CO) at low concentration (100-300 ppb) due to high surface area. By combined three nanowires sensors, the microelectronic nose has great potential to detect and discriminate a wide variety of gases including toxic gases and non-toxic gases.

Acknowledgments

This work was supported by a grant (TRF-CHE-KU Research Grant for New Scholar) from Thailand Research Fund, Commission on Higher Education and Kasetsart University Research and Development Institute (MRG 5580229).

References

[1] G. C. Green, A. D. C. Chan and M. Lin, *Sens. Actuators B,* 2014, **190**, 16-24.

[2] C. Wongchoosuk, A. Wisitsoraat, A. Tuantranont and T. Kerdcharoen, *Sens. Actuators B,* **147**, 392-399.

[3] T. Carvalho, P. Vidinha, B. R.Vieira, R.W. C. Li and J. Gruber, *J. Mater. Chem. C*, 2014, **2**, 696-700.

[4] E. A. Baldwin, J. Bai, A. Plotto and S. Dea, *Sensors*, 2011, **11**, 4744-4766.

[5] W. Ko, N. Jung , M. Lee , M. Yun and S. Jeon, *ACS Nano*, 2013, **7**, 6685–6690.

[6] N. S. Ramgir, Y. Yang and M. Zacharias, *Small,* 2010, **6**, 1705–1722.

[7] P. C. Chen, F. N. Ishikawa, H. K. Chang, K. Ryu and C. Zhou, *Nanotechnology*, 2009, **20,** 125503.

[8] J. M. Baik, M. Zielke, M. H. Kim, K. L. Turner, A. M. Wodtke and M. Moskovits, *ACS Nano*, 2010, **4**, 3117-3122.

[9] C. Wongchoosuk, K. Subannajui, A. Menzel, I. Amarilio-Burshtein, S. Tamir, Y. Lifshitz and M. Zacharias, *J. Phys. Chem. C*, 2011, **115**, 757-761.

[10] Y. Yang, D. S. Kim, M. Knez, R. Scholz, A. Berger, E. Pippel, D. Hesse, U. Gösele and M. Zacharias, *J. Phys. Chem.* C, 2008, **112**, 4068–4074**.**

[11] K. Keem, H. Kim, G. T. Kim, J. S. Lee, B. Min, K. Cho, M. Y. Sung and S. Kim, *Appl. Phys. Lett.*, 2004, **84**, 4376-4378.

[12] J. Chen, K. Wang, R. Huang, T. Saito, Y. H. Ikuhara, T. Hirayama and W. Zhou, *IEEE Trans. Nanotechnol.*, 2010, **9**, 634-639.

[13] S. N. Bai and S. C. Wu, *J. Mater. Sci.: Mater. Electron.*, 2011, **22**, 339–344.

[14] Q. Wan, Q. H. Li, Y. J. Chen, T. H. Wang, X. L. He, J. P. Li and C. L. Lin, *Appl. Phys. Lett.*, 2004, **84**, 3654- 3656.

[15] J. B. K. Law and J. T. L. Thong, *Nanotechnology*, 2008, ***19***, 205502.

[16] S. Chang, I. M. Vitomirov, L. J. Brillson, D. F. Rioux, P. D. Kirchner, G. D. Pettit, J. M. Woodall and M. H. Hecht, *Phys. Rev. B*, 1990, **41**, 12299-12302.

[17] S. W. Fan, A. K. Srivastava and V. P. Dravid, *Appl. Phys. Lett.*, 2009, **95**, 142106.

[18] J. Zhao, T. Yang, Y. Liu, Z. Wang, X. Li, Y. Sun, Y. Du, Y. Li and G. Lu, *Sens. Actuators B*, 2014, **191**, 806–812.

[19] R. Revel, D. Bazin, P. Parent and C. Laffon, *Catal. Lett.*, 2001, **74**, 189- 192.

[20] S. Park, S. An, Y. Mun and C. Lee, *ACS Appl. Mater. Interfaces*, 2013, **5**, 4285−4292.

[21] Y. C. Liang and W. K. Liao, *RSC Adv.*, 2014, **4**, 19482-19487.

[22] H. Dixit, N. Tandon, S. Cottenier, R. Saniz, D. Lamoen and B. Partoens, *Phys. Rev. B,* 2013, **87**, 174101.

[23] V. V. Sysoev, J. Goschnick, T. Schneider, E. Strelcov and A. Kolmakov, *Nano Lett.,* 2007, **7**, 3182-3188.

Lists of Figures

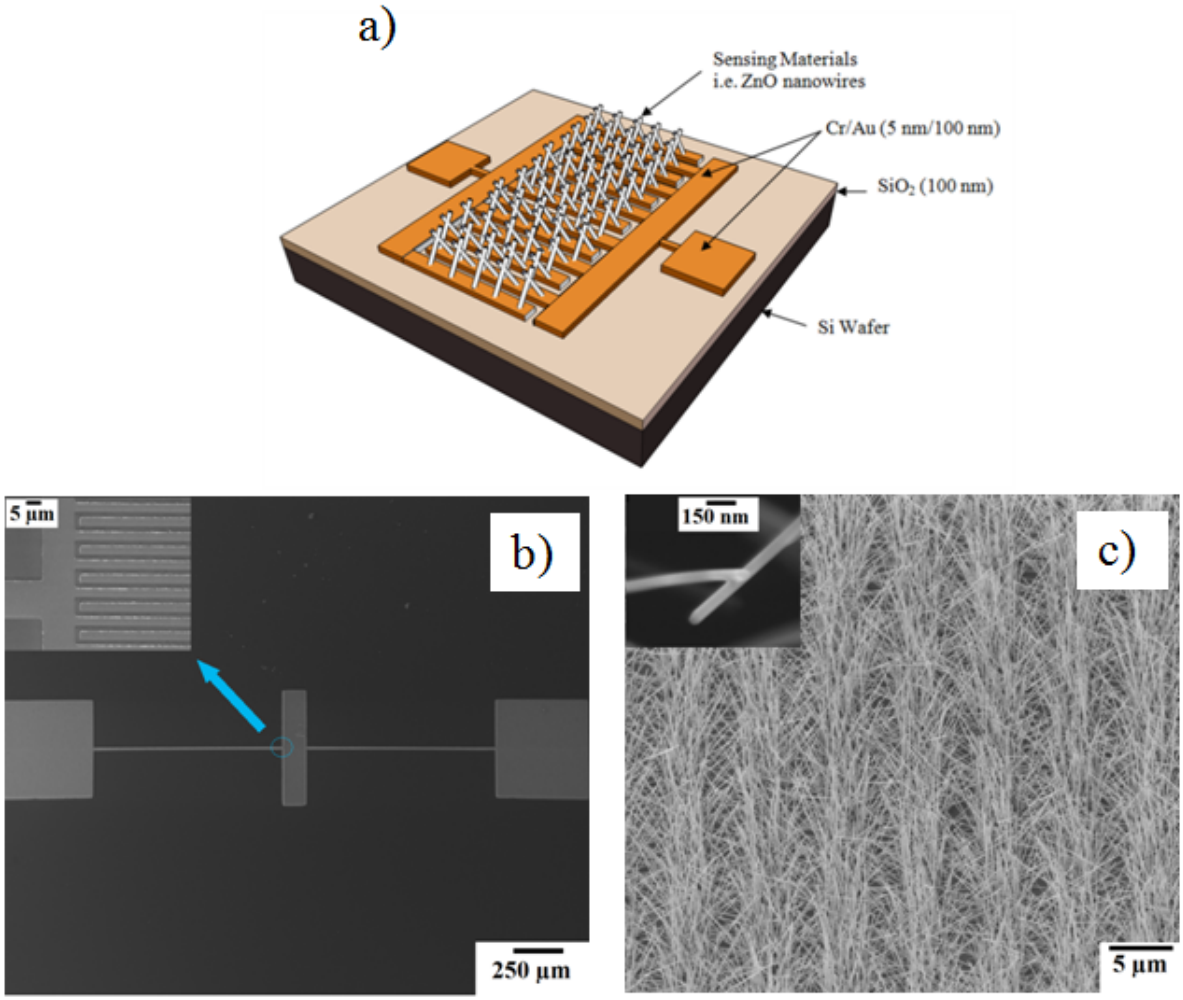

Figure 1

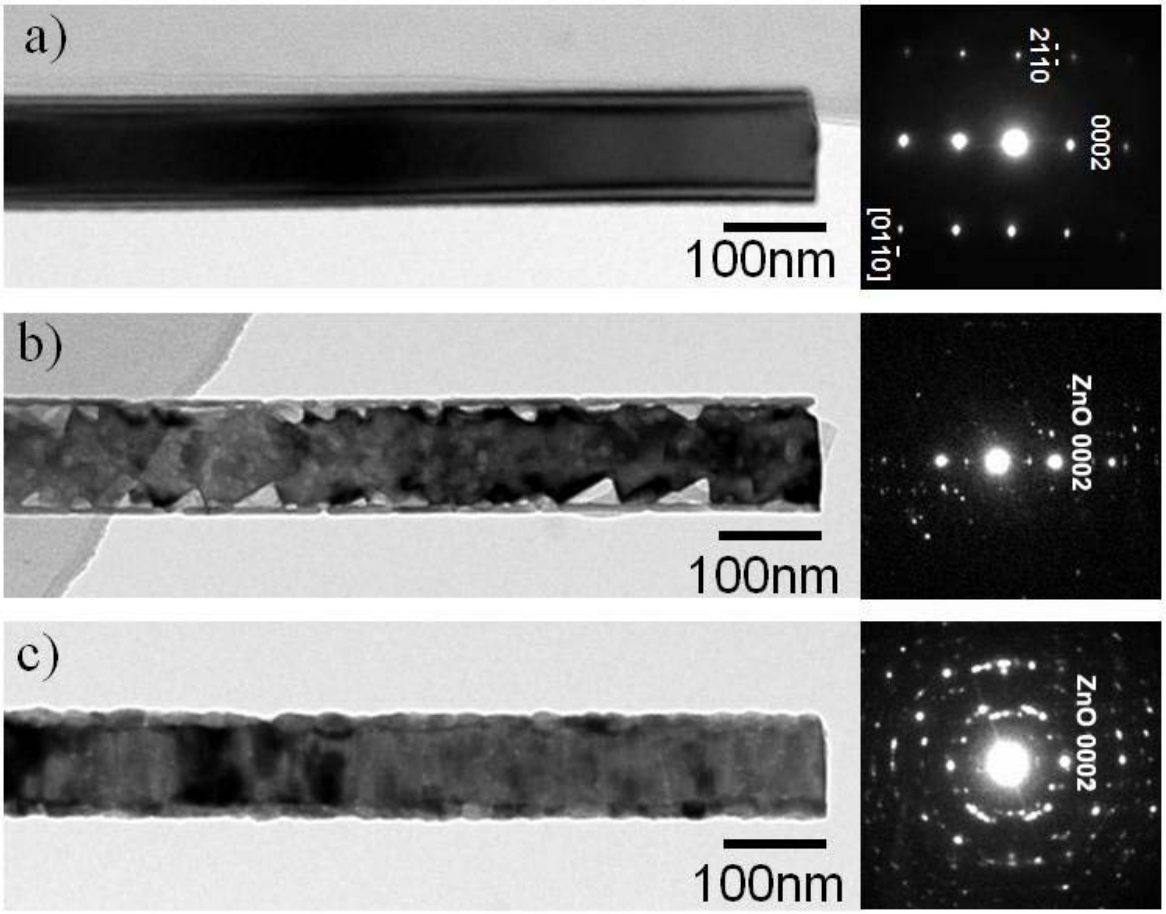

Figure 2

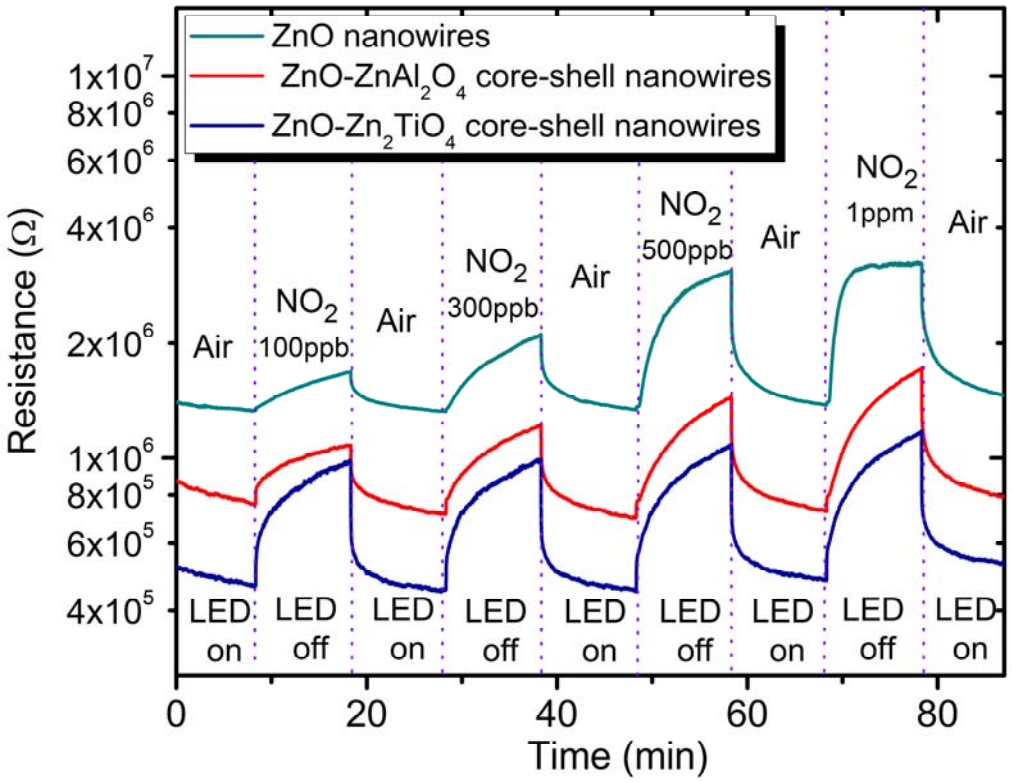

Figure 3

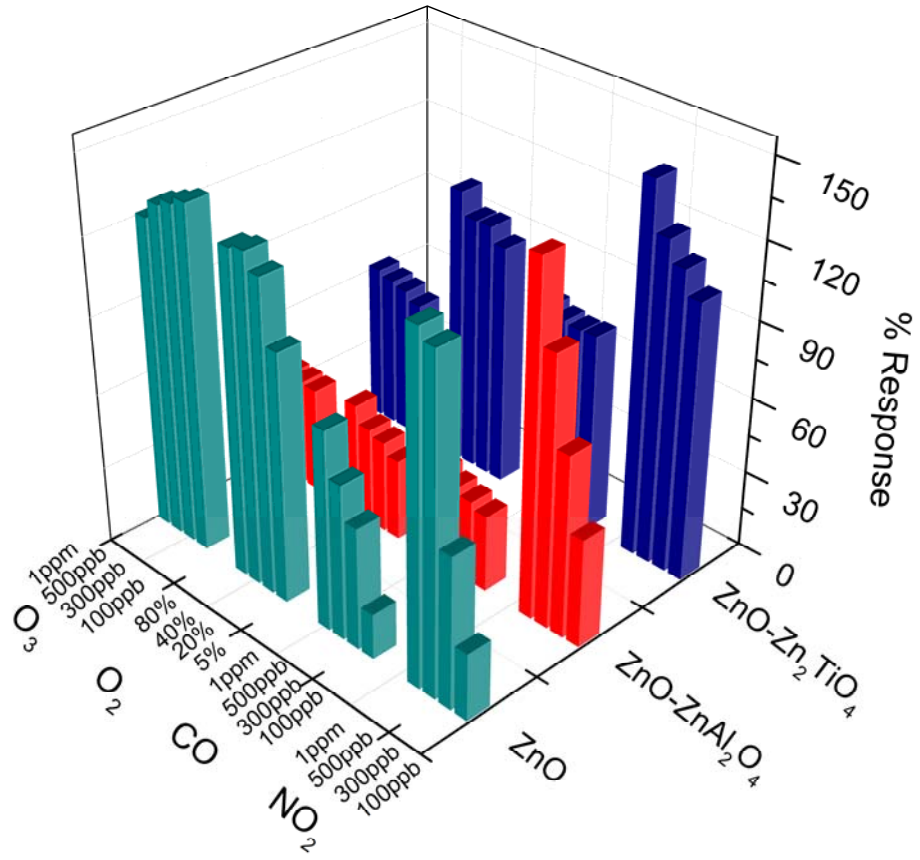

Figure 4

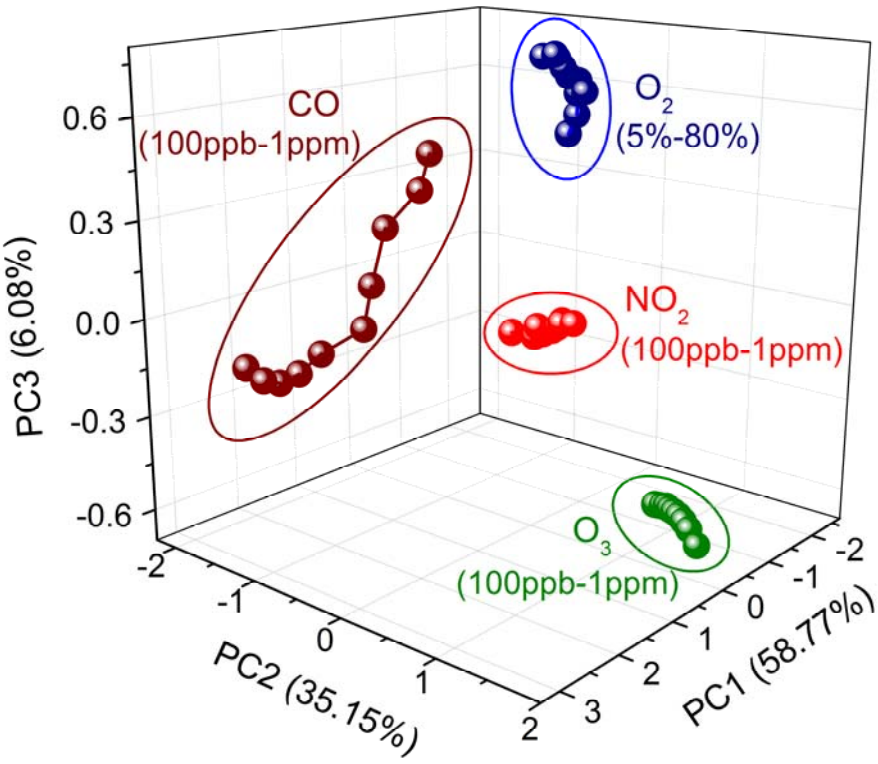

Figure 5